IN-SITU ACOUSTIC EMISSION MONITORING OF ACCELERATED CORROSION OF WROUGHT IRON

Kutsi Akcicek[1)], Sinan Acikgoz[1)] and Heather Viles[2)]
1) Department of Engineering Science, University of Oxford, Oxford, United Kingdom
2) School of Geography and the Environment, University of Oxford, Oxford, United Kingdom

ABSTRACT: Wrought iron bars, with attached waterproofed acoustic emission (AE) sensors, were subject to accelerated degradation in a corrosion chamber. During the transition from the wet to dry stages of the sample, a significant rise in AE hits was observed. Conversely, in fully dry or wet stages, fewer AE hits were detected. Based on the AE activity between transition stages, the results support existing theories of atmospheric corrosion of iron and the significance of wet to dry cycles in this process. Waterproofing of sensors for *in-situ* corrosion studies has also shown to be viable without causing damage to the sensor itself.

1 INTRODUCTION

Wrought iron is a material that was commonly used in architectural contexts as a reinforcement or strengthening material. It is a composite material consisting of an iron matrix with interspersed slag inclusions. Slag consists mainly of glass, and incorporates materials from the iron manufacturing process from the ore, gangue, kiln, tuyeres, *etc*. Iron that is embedded in buildings was typically surrounded by a layer of lead, which was poured in its molten state. This had two purposes: it first set the iron in place as the lead solidified around it, and secondly it also provided corrosion resistance as the lead acted as a physical barrier to water and oxygen ingress. This lead can, however, be removed, or was never introduced in the first place, and thus no longer provides a barrier to corrosion. Where corrosion of iron in buildings occurs, the corrosion products will cause the volume of the reinforcement to increase, and impart stress to the surrounding masonry as it grows. These stresses can then lead to the cracking of the masonry, which creates potential structural and aesthetic problems, especially in heritage buildings.

Atmospheric corrosion of iron, which is a prevalent form of corrosion for reinforcements, involves the repeated wet-dry cycling of iron. Cyclic corrosion of iron has been studied and proposed theories exist regarding the process itself [1,2]. Experimental work regarding the atmospheric corrosion of iron showed that the maximum corrosion rate occurs at the intersection of a wet-dry stage [1]. An electrolytic layer of water exists on the surface of the iron which changes in thickness depending on the stage of the wet-dry cycle [2].

In the current literature, acoustic emission (AE) monitoring has been used by other researchers to study the corrosion of iron and steel [3–6]. These experiments mainly used galvanostatic methods of corrosion to accelerate the corrosion damage. Several different forms of corrosion can be successfully monitored using AE sensors including uniform and pitting. However, galvanostatic methods may not be truly representative of real-world scenarios, and may produce different corrosion products compared to other methods [7]. Another alternative method is the use of accelerated corrosion chambers to induce corrosion. Little research has been undertaken where AE sensors are used *in-situ* in corrosive environments to record damage mechanisms. This would require sensors that are adapted to harsh environments, where the material being monitored must be corroded, but the sensor itself must resist corrosion. To this end, this paper explores the use of waterproofing techniques to ensure that AE sensors can monitor corrosion of iron in-real-time, when this corrosion is carried out in an accelerated corrosion chamber. This paper also offers the opportunity to monitor the cyclic corrosion of iron using non-electrochemical methods.

2 METHODS

Wrought iron bars were purchased from Topp & Co (Tholthorpe, United Kingdom). This is the last commercial producer of wrought iron in the United Kingdom, who re-roll previous bars of wrought iron. From larger bars, four pieces of iron were cut and reduced in size down to approximately 23 x 5.1 x 1.3 cm. No additional sample preparation was undertaken on the iron.

A Mistras Micro-SHM system with four narrow-band resonant R6α sensors was used, with each sensor possessing a 26 dB external amplifier. To waterproof the sensors, a layer of Thermoworx Whitemorph® thermosetting plastic was first applied to the sensors, ensuring that any cable connection screws were left untouched. To avoid water being in contact with the sensors, the thermoplastic was melted in a metal container which was placed into a waterbath at 90 °C. Additionally, a layer of polyolefin shrink tubing was inserted around the wire before being heated with a heatgun to shrink it around the original wire. After, the AE sensor was positioned onto the sample, a thick layer of OTTO-CHEMIE OTTOSEAL S18 silicone sealant was applied between the sensor and the iron, acting as a couplant, as well as all around the sensor and partly along the wire, for waterproofing. This specific sealant was chosen as it was neutral curing, meaning it does not release acidic products during setting, and

so would cause limited damage to the sensor. Secondly, the sealant is specially designed for chlorinated environments, meaning it would offer suitable protection in an accelerated corrosion chamber. A threshold of 40 dB was used to filter out background noise which may be detected by the AE sensors. Data with a recorded duration of 0 µs was filtered out of the dataset as they are assumed to be spurious data.

Accelerated atmospheric corrosion of the samples occurred in an Ascott CC450iP corrosion chamber (Figure 1). To corrode the sample, a slightly modified version of BS EN IEC 60068-2-52:2018 Method 7 [8] was used (Figure 2). This method is a three-stage process which involves a salt spray period (Stage 1), followed by a hot period (Stage 2), and ends with a humid period (Stage 3), before cycling back to salt spray and repeating. For the salt spray, a 5% NaCl solution was used. Each cycle lasted for 8 hours. The temperature used in Stage 2 of the corrosion was lowered from 60 °C (in the standard) to 58 °C (in the experiment). This is because the Thermoworx melts at 62 °C, and the lowering of the Stage 2 temperature was taken as a precaution to avoid any potential melting during the experiment. Additionally, Stage 2 was split into Stage 2a and 2b to ensure that the transition to Stage 3 would be within the time limits of the standard. Stage 2a had the humidity set to as low as possible, whereas Stage 2b was set to 27% RH—both being less than the 30% RH required for Stage 2 in the standard. The samples were corroded for 60 cycles, which coincided with 20 days inside the corrosion chamber.

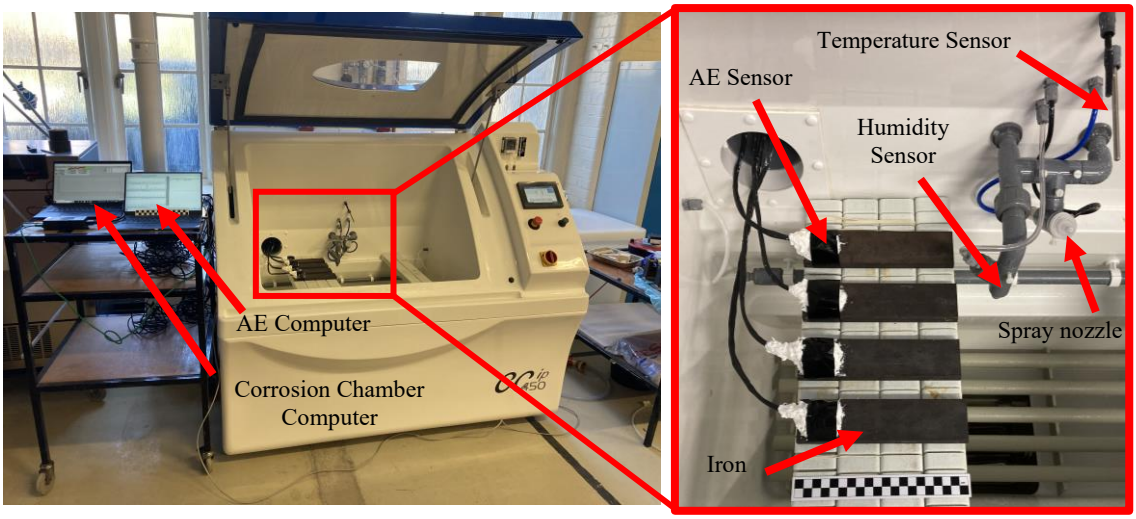


Figure 1: Labelled experimental set-up of combined AE and corrosion chamber experiment prior to the beginning of the experiment. Scale bar is 20 cm.

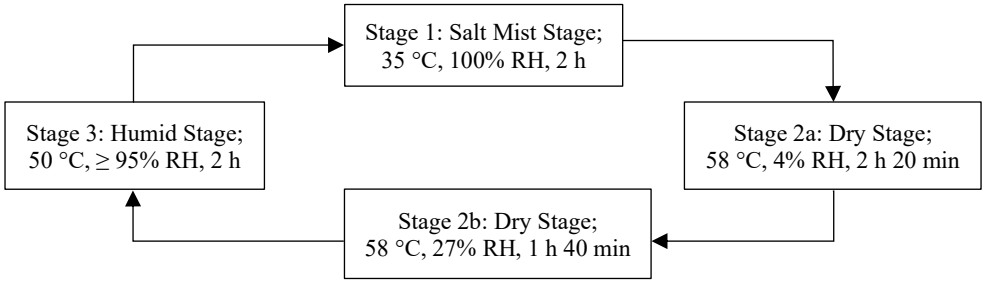


Figure 2: Modified version of BS EN IEC 60068-2-52:2018 Method 7 which was utilized for this study.

3 RESULTS

Several thousands of AE hits were recorded in Stage 1 of the corrosion cycle from the moment the salt spray turned on. These are most likely from the droplets of salt spray falling onto the sample and being detected by the sensors. Therefore, any data from Stage 1 in all 60 cycles is not considered to be related to corrosion in the iron and was discarded in any further data analysis. Additionally, a computer error meant that AE data was not recorded for Stages 2a, 2b, and 3 of Cycle 20. In certain cycles (Cycles 33–36, 48, 50, and 57) the humidity sensor cap became covered with salt and the humidity control of the chamber did not work as expected. In these cycles, a slightly different observation occurred, as discussed below. Additionally, for Iron 1, the number of cumulative AE hits in all stages of Cycle 19 was anomalously high, but not in other samples; it is not known why this occurred. Data from Cycles 19, 33–36, 48, 50, and 57 have still been included in this study for further processing.

Observations of the corrosion surface showed that from the end of Cycle 1, localised pockets of corrosion were forming. After further cycles, a uniform corrosion layer formed across the entirety of the sample and was noted to

increase in thickness throughout the course of the experiment (Figure 3). Further cycles caused bulges to form in the corrosion layer, before several of these bulges split down the middle. The deposition, growth, and subsequent splitting and cracking of the oxide layer would have likely acted as sources of AE hits, alongside the dissolution of the iron during the corrosion process itself.

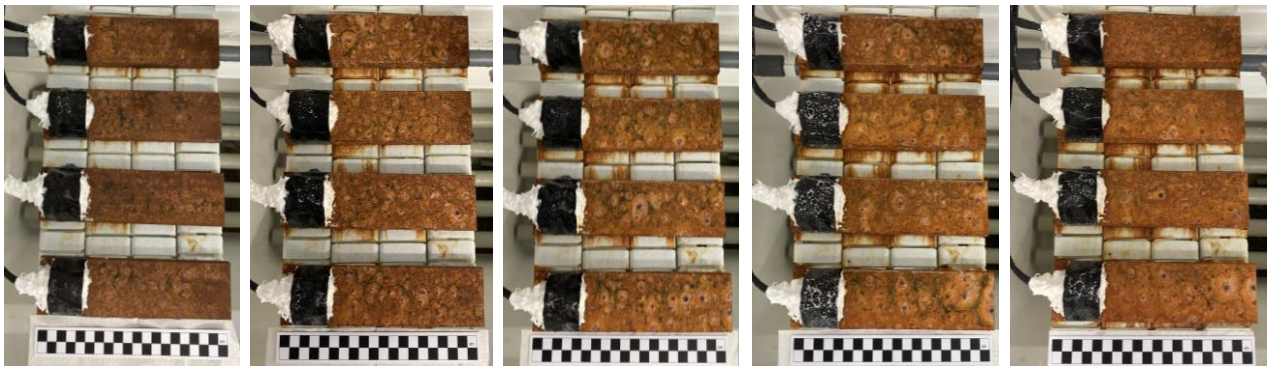


Figure 3: Evolution of corrosion layer on samples. Left to Right: Day 4, 9, 12, 17, and 20. Scale bar is 20 cm.

When the experiment was over, the silicone was removed from the sensor using manual cutting. Akin to how it was placed there in the first instance, the thermosoftening plastic was removed by placing the sensor into a metal tray which was placed in a water bath. No visible damage or corrosion products were detected on the sensor itself.

3.1 *Intra-cycle*

Within a single cycle, where the sensor cap was free of salt deposition, a similar pattern of detected cumulative AE hits was observed throughout each cycle (see Figure 4 for an example of this pattern). Two major increases in AE hits are observed within a single cycle: during Stage 2a and the transition from Stage 2b to 3. There is a much smaller increase in the number of signals detected during Stage 2b, compared to the previous rise in Stage 2a. Finally, there are hardly any signals detected in Stage 3. In some samples, the last detected signal is significantly before the end of Stage 3. This pattern was consistently observed across all four tested irons. When salt deposition occurred on the humidity sensor, the humidity did not decrease gradually, but instead decreased in an oscillating manner between Stages 1 and 2a and 2b. This led to very large increases in the detected AE hits especially during Stage 2b, before decreasing again during Stage 3.

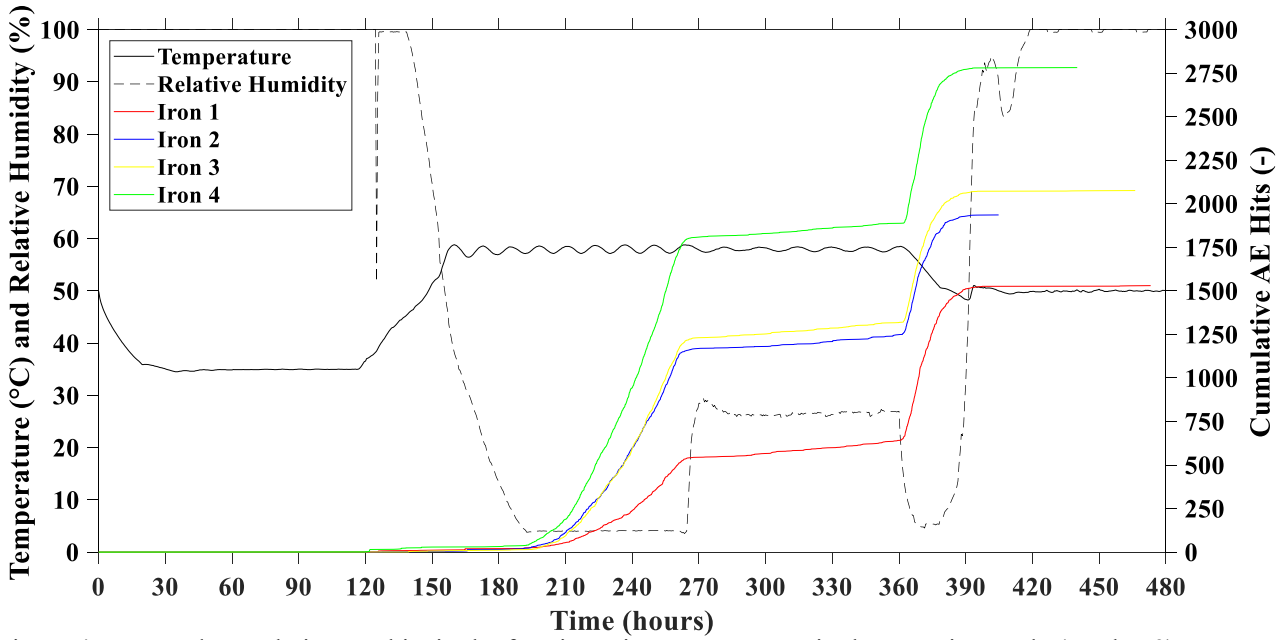


Figure 4: Detected cumulative AE hits in the four irons in response to a single corrosion cycle (Cycle 59).

3.2 *Inter-cycle*

Between different cycles, the number of cumulative AE hits in a single cycle increased up until roughly halfway through the experiment (~6000 hits around Cycle 30), before beginning to decrease after this (Figure 5). When

comparing the number of hits in each stage, the same relationship is not followed consistently. The number of cumulative AE hits detected in Stage 2a and 2b shows a similar relationship to the overall trend (increased until halfway through the experiment and then decreased). The number of cumulative AE hits detected in Stage 3 increased throughout the course of the experiment, before beginning to plateau nearer the end.

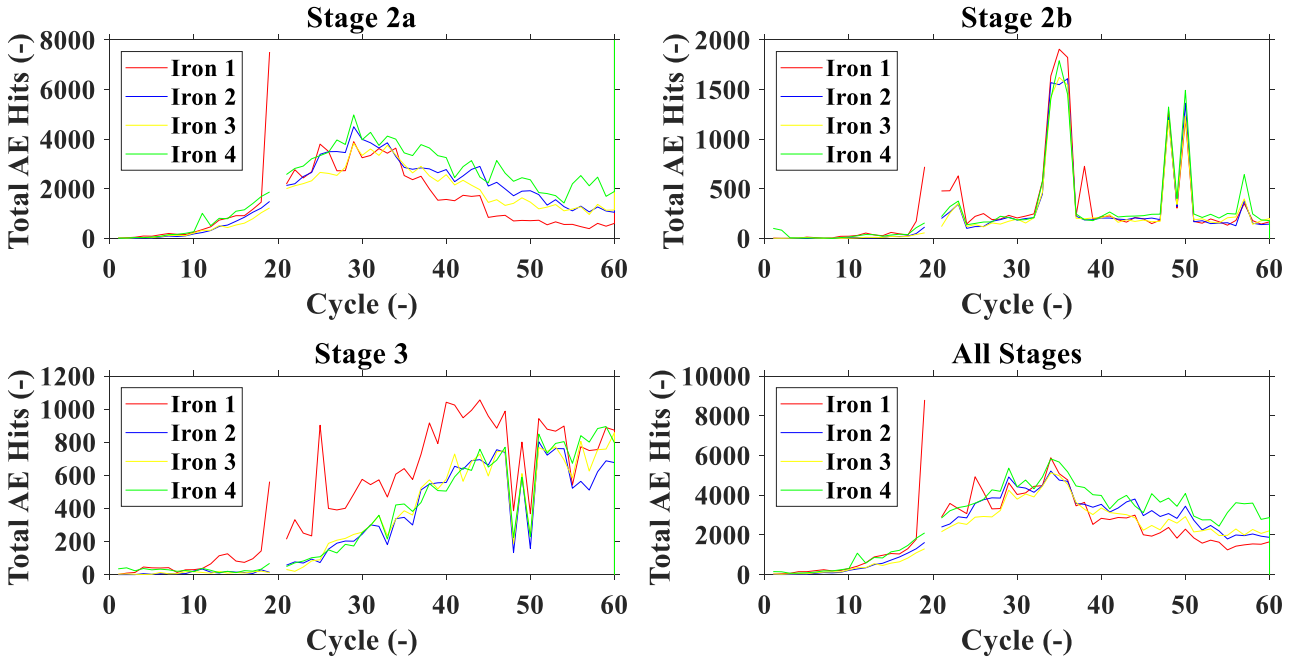


Figure 5: Detected AE hits in the four irons across each stage of the experiment, as well as their combined value for each cycle.

The average and maximum amplitude of the AE hits was observed to generally increase over the course of the experiment, in all four irons (Figure 6). Maximum values roughly in the range of 40–60 dB were observed during the first 100 hours, before a gradual increase to maximum values above 80 dB after 200 hours of the experiment.

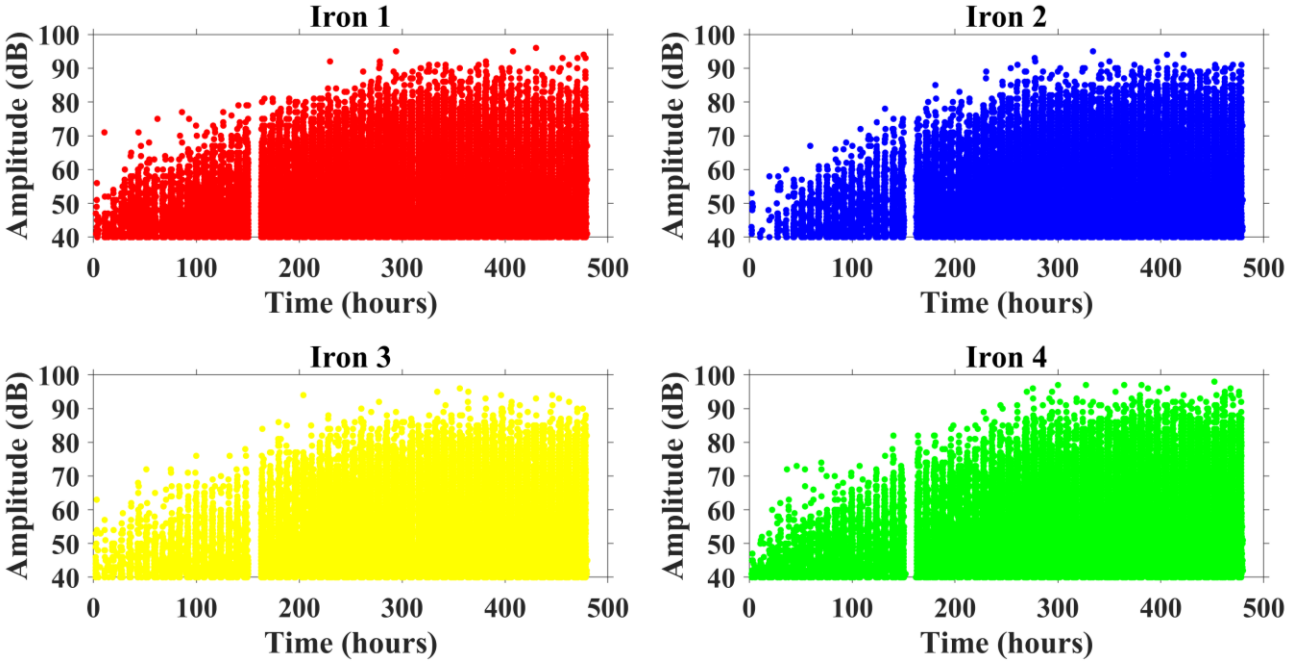


Figure 6: Distribution of detected AE amplitudes in the four irons across the duration of the experiment.

4 DISCUSSION

4.1 *Intra-cycle*

The first major increase in AE hits likely coincides with the drying of the sample. There is a lag between the corrosion chamber increasing in temperature from 37 °C to 58 °C and the recorded increase in AE hits. This likely

occurs because it takes time for the sample to also be heated sufficiently to cause the transition from wet to dry. The rate of AE hits is initially high when the sample begins to dry out, but the rate decreases during Stage 2a as the sample evaporates and the sample becomes fully dry. During Stage 2b, the number of AE hits produced decreases, but there is still some production of AEs. An increase of humidity from 4% to 27% likely caused a small electrolytic layer to form on the sample. However, the high temperature would have likely caused it to evaporate, but this could have been replaced with further water vapor that is present in the chamber. This would have likely led to the sample undergoing continuous wet-dry cycles, with an electrolyte layer of varying thickness. The layer, however, would not have been large as Stage 2a, hence why the magnitude of AE hits is not as large. The second major increase in AE hits occurs between the transition from Stage 2b to 3. The corrosion chamber did not transition from 27% RH to 95+% RH in one step. Instead, it expelled all humidity from the chamber to 4% RH before then increasing to 95+% RH. As the temperature is still warm, there is no lag in time to detect a large increase in AE, which is what occurred in Stage 2a as the sample was originally heating up. Thus, the temporary reduction in humidity likely caused a second wet-dry cycle in the sample. When the sample reached Stage 3, the humidity was at a maximum, and the temperature decreased slightly. The high relative humidity at this stage likely caused a thick permanent electrolyte layer to form on the sample. Thus, the material did not experience any further wet-dry cycles and hence why the least amount of AE hits were detected in this stage. Even if the temperature was warm enough to cause evaporation, the very high humidity meant that the surface electrolyte layer never dried up sufficiently to cause corrosion noise.

The occurrence of increases in cumulative AE hits at the regions where wet-dry cycles occur provides non-electro-chemical evidence that current proposed theories do capture the corrosion mechanisms that occur in wrought irons. Whilst it was not possible to directly measure these results electro-chemically, AE sensors have proven to be a useful method in monitoring the corrosion of ferrous samples.

4.2 *Inter-cycle*

Focusing on Stage 2a across different cycles, there is an increase in the number of hits until there is a maximum around halfway through the experiment. After this point, a decrease occurs before the value plateaus. The initial increase is likely due to the initial corrosion of the sample and deposition of the oxide layer. Loss of metal and any signals associated with micro-cracking and delamination of the oxide layer will have likely generated noise. The decrease in the number of cumulative hits partway through the experiment may have occurred as the thickness of the corrosion layer began to increase beyond a critical value. It would then become increasingly difficult to completely dry the sample and conduct full wet-dry transitions. Thus, there is likely a diffusion-related factor which governs the corrosion response of the irons. Noise generated during Stage 2b is from a similar mechanism as those from Stage 2a. AE signals from Stage 3 follow a different trend, where the number of AE hits is increasing further into the experiment before plateauing. These signals are not caused by wet-dry cycles, and may instead be caused by the cracking of the oxide layer. As it grows in thickness during the experiment, more signals are detected, hence why the maximum AE hits in per cycle in Stage 3 does not coincide with the other two stages.

During Stage 2b, where humidity lowered in an oscillating manner due to a salt-encrusted humidity sensor, the AE hits were significantly higher. The oscillating nature of the humidity, coupled with the high temperature, likely meant that constant wet-dry cycles were occurring within the specimen, which caused a higher proportion of signals to be produced than expected if the humidity was lowered just once.

Increases in amplitude during corrosion studies have been previously correlated with the growth and cracking of oxide scales during repeated thermal cycling [9]. As a similar mechanism has been observed during this experiment, this phenomenon has likely occurred here. The oxide layer grew in thickness over the experiment and then cracked, which was also observed visually with the splitting open of bulges.

5 CONCLUSION

Architectural wrought iron is subject to corrosion inside buildings which causes damage as the iron expands in volume due to the growth of an oxide layer. Current theories regarding the corrosion of iron postulate that the rate of corrosion occurs at a maximum when a wet sample begins to dry. To investigate this process, four samples of wrought iron were subject to accelerated corrosion in a corrosion chamber whilst being monitored using waterproofed AE sensors. A four-stage corrosion methodology was selected to investigate this, which involved the spraying of samples with 5% NaCl solution, followed by subsequent drying in a hot environment and wetting in a humid environment. The specific methodology used involved two wet-dry transitions. The following major findings were observed:

- The largest increases in detected AE hits occurred at the intersection of the two wet-dry cycles, coinciding with the most significant corrosion period of the irons. Stages where wet-dry transitions were not occurring

coincided with less AE activity. The results of this study provide further evidence for current theories regarding the cyclic corrosion of irons.

- The maximum detected amplitude of the AE hits increased gradually over time, suggesting that the development and cracking of the oxide layer is a significant emitter of AE signals during this experiment due to a mixture of wet-dry cycles and thermal cycling.
- This study has also shown that *in-situ* AE analysis of corrosion processes conducted in an environmental chamber can be viable when waterproofing of AE sensors is undertaken. For the purposes of this study, this was achieved using a double layer of thermosoftening plastic following by chlorine-resistant neutral setting silicone sealant. Additional waterproofing of the wires was achieved by heating shrink tubing plastic around them. No visible damage was recorded on sensors after removal of the waterproofing materials.

Monitoring degradation processes *in-situ* using AE in a corrosion chamber allowed for further understanding of degradation mechanisms in iron. This study has also shown that longer-term corrosion monitoring of iron objects, either architecturally or otherwise, can be achieved where waterproofing of AE sensors has also been undertaken. Further experiments on other material types subject to degradation can also be undertaken, where there is sufficient waterproofing of sensors.

6 ACKNOWLEDGEMENTS

The authors would like to thank Mr Clive Baker for practical assistance in installing and maintaining the corrosion chamber. This research was undertaken as part of doctoral study of the lead author and was supported by the Engineering and Physical Science Research Council (EPSRC) Grant No. EP/T517811/1 and EP/W524311/1.

7 REFERENCES

[1] Stratmann, M. & Streckel, H., 1990. “On the Atmospheric Corrosion of Metals Which Are Covered with Thin Electrolyte Layers—II. Experimental Results.” *Corrosion Science*, Vol.30, Iss.6–7, pp.697–714.

[2] Hœrlé, S., Mazaudier, Ph., Dillmann, P. & Santarini, G., 2004. “Advances in Understanding Atmospheric Corrosion of Iron. II. Mechanistic Modelling of Wet–Dry Cycles.” *Corrosion Science* Vol.46, Iss.6, pp.1431–1465.

[3] Seah, K. H. W., Lim, K. B., Chew, C. H. & Teoh, S. H., 1993. “The Correlation of Acoustic Emission with Rate of Corrosion.” *Corrosion Science* Vol.34, Iss.10, pp.1707–1713.

[4] Kim, Y. P., Fregonese, M., Mazille, H., Fèron, D. & Santarini, G., 2003. “Ability of Acoustic Emission Technique for Detection and Monitoring of Crevice Corrosion on 304L Austenitic Stainless Steel.” *NDT&E International* Vol.38, Iss.8, pp.553–562.

[5] Jirarungsatian, C. & Prateepasen, A., 2010. “Pitting and Uniform Corrosion Source Recognition Using Acoustic Emission Parameters.” *Corrosion Science* Vol.52, Iss.1, pp.187–197.

[6] Livadiotis, S., Sitaropoulos, K., Ebrahimkhanlou, A. & Salamone, S., 2023. “Acoustic Emission Monitoring of Corrosion in Steel Pipes Using Lamb-type Helical Waves.” *Structural Health Monitoring* Vol.22, Iss.2, pp.1225–1236.

[7] Yuan, Y., Ji, Y. & Shah, S. P., 2007. “Comparison of Two Accelerated Corrosion Techniques for Concrete Structures.” *ACI Structural Journal* Vol.104, Iss.3, pp.344–347.

[8] BS EN IEC 60068-2-52:2018., 2018. *Environmental Testing. Part 2: Tests – Test Kb: Salt Mist, Cylic (Sodium Chloride Solution)*.

[9] Christl, W., Rahmel, A. & Schütze, M., 1987. “Application of the Acoustic Emission Technique for the Detection of Oxide Scale Cracking During Thermal Cycling.” *Materials Science and Engineering* Vol.87, pp.289–293.